Production Engineering (2022) 16:453–463
https://doi.org/10.1007/s11740-021-01090-y

MACHINE TOOL

Experimental investigation into the implications of transmission errors for rack-and-pinion drives

Lukas Steinle[1] · Armin Lechler[1] · Michael Neubauer[1] · Alexander Verl[1]

Received: 27 August 2021 / Accepted: 22 November 2021 / Published online: 29 November 2021

Abstract
Rack-and-pinion drives are the preferred option in the machine tool sector when long ranges of motion and high loads are involved. However, their shortcomings particularly include deficiencies in the achievable positioning and path accuracy. The backlash as one of the main issues is well described in the literature and numerous solutions to reduce its negative effects exist. In contrast, there is a lack of literature regarding the scientific and systematic analysis of the transmission errors in rack-and-pinion drives. In this paper, the displacements originating in the drive train of a system with industrial components are measured under different operating conditions. The observed transmission errors are thoroughly analyzed in no-load operation and their sources are discussed. Subsequent investigations show significant load-dependent alterations of the transmission errors and direction-dependent characteristics, the causes of which are explained. It is shown, that transmission errors negatively affect the path accuracy of position controlled drives, which is amplified by excitation of the machine structure in certain operating conditions. To address this issue, different error compensation concepts are presented.

Keywords Rack-and-pinon · Feed drive · Transmission errors · Path accuracy · Machine tools

1 Introduction

Modern manufacturing equipment is expected to deliver high production quality coupled with high dynamic performance. Both properties are largely determined by the installed drive systems. In addition to the achievable feed forces, they also define the accuracy and the static and dynamic rigidity. Rack-and-pinion drives (RPDs) are the preferred choice for applications with long travel distances and high loads [1]. The stiffness of these drive systems is independent of the travel distance and since only stationary rack elements are added to increase the axis length, whereas the inertia moved by the drive remains unchanged, arbitrarily long travels can be realized without inhibiting the dynamics [2]. This high scalability in combination with economical implementation make RPDs particularly suitable for heavy machinery [3]. Nevertheless, they also have some specific downsides. Of particular relevance for machine tools is the inferior positioning and path accuracy compared to other drive types [2]. A major issue limiting the positioning accuracy is backlash, which has a negative effect on both static and dynamic performance. However, the literature offers various approaches to eliminate its negative effects to a great extent by utilizing mechanical [3] or electrical [4] preload or designated model-based control strategies [5], that can also factor in elasticity [6].

In consequence, other sources of error become more apparent. One issue that mainly influences the dynamic accuracy and causes deviations during trajectory tracking is the transmission error (TE) of RPDs. TEs are defined as the deviations of position and velocity that occur between the input and output of gearings [7]. In the case of RPDs, such errors are present both in the meshing of the rack and pinion and in other gearing in the drive train. The result are periodic position differences between the drive motor and the table that can lead to vibration excitation and unsatisfactory surface finish of the workpieces. TEs are comprehensively described for gearwheel pairings [8], including vibration research [9], their minimization through design improvements [10] and implications for planetary gears [11]. For rack-and-pinion gearings literature regarding simulative studies utilizing FEM tools [12] as well as analytical

✉ Lukas Steinle
lukas.steinle@isw.uni-stuttgart.de

[1] Institute for Control Engineering of Machine Tools and Manufacturing Units (ISW), University of Stuttgart, Seidenstrasse 36, 70174 Stuttgart, Germany

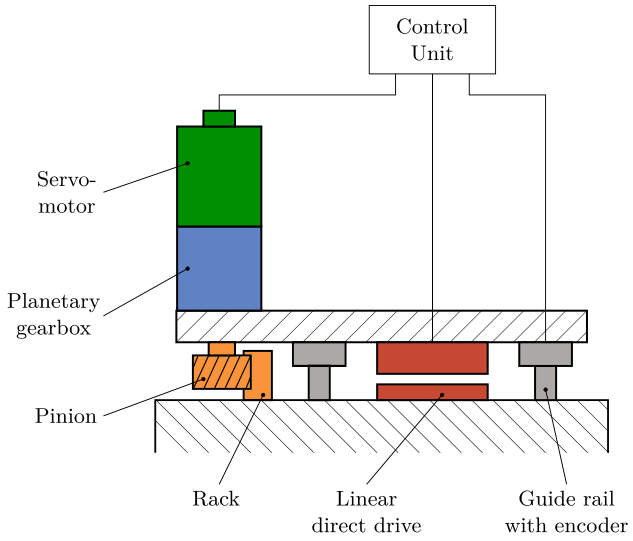

Fig. 1 Architecture of the rack-and-pinion test bench

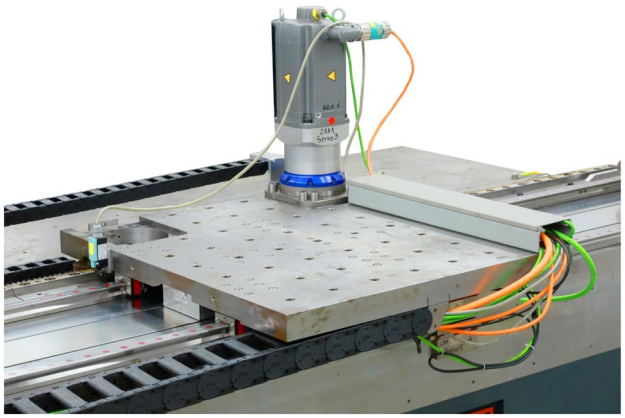

Fig. 2 Picture of the utilized test bench

Table 1 List of the components used in the test bench

Component	Manufacturer	Factory number
Synchronous motor	Siemens	1FT708
Motor encoder	Siemens	AM24DQI
Planetary gearbox	Wittenstein	RP040S
Pinion	Wittenstein	RMT400
Rack	Wittenstein	ZST400
Linear direct drive	Siemens	1FN3300
Guide rails	Schneeberger	AMSABS3
Control unit	Siemens	CU320-2-DP

Table 2 Relevant parameters of the RPD and other test bench components

Parameter	Symbol	Value	Unit
Helix angle	β	19.5283	°
Pressure angle	α_n	20	°
Pitch diameter	d_p	84.882	mm
Pinion teeth	z	20	–
Gearbox ratio	i_{PG}	16	–
Table mass	m_T	420	kg
Position control gain	K_v	70.8	1/s
Velocity control gain	K_p	6.65	Nms/rad
Velocity control Time constant	T_n	2.26	ms

models [13] exist. In addition, studies concerning automotive steering systems [14] and variable compression combustion engines [15] are available. However, in the context of position-controlled feed drives with RPD, there is hardly any literature to date that provides experimental data concerning the impact of TEs on the path accuracy and vibration excitation of the drive mechanics. As a consequence, approaches for their compensation are uncommon. This paper is intended to contribute to adress this gap.

Therefore in Sect. 2 a setup with industrial components for experimental investigation is presented. Section 3 analyzes the TEs of this RPD in detail under different operating conditions. Following this, the effects on the path accuracy of the controlled drive are examined in Sect. 4, involving the elaboration of potential excitations of the machine structure induced by the drive train in Sect. 4.1. Subsequently concepts to compensate for the deviations from a control engineering perspective are presented in Sect. 5.

2 Experimental setup

To investigate the transmission uniformity of RPDs, an exemplary system that is comparable to common industrial implementations is used as a test bench. Figure 1 outlines the schematic structure of such a system with RPD and Fig. 2 shows a picture of the corresponding test bench utilized in this paper.

The servomotor actuates the pinion through a high-precision two-stage planetary gearbox. The linear motion is subsequently provided through the meshing of pinion and rack. To enhance smoothness of movement, gearing with a helix with an incline β of 19.5283° is used. The drive is guided by two guide rails and the mass m_T of the table with the drive system is 420 kg. The components used are listed in Table 1 and relevant parameters can be taken from Table 2.

A specific feature of the test bench is a linear direct drive (LDD) mounted in the center of the table in parallel to the feed drive. This allows to apply forces to the RPD and thereby simulate loads.

The central control unit is a Siemens CU320-2 with corresponding inverters for motor and LDD. The position control of the drive is done by a cascade control. Figure 3 illustrates such a configuration, as it is used in the setup under consideration. The structure consists of three interconnected control loops [16]. While the innermost current control loop has negligible influence on the system characteristics, the velocity and position control loops are decisive for the properties of the drive [17]. The velocity controller regulates the rotational velocity of the drive motor $\dot{\theta}_M$ via the desired motor torque T_s. The position controller, obtaining the target position x_s, provides the desired table velocity v_s. In case of an indirect position control the control loop is closed through feedback of the motor position x_M. While this configuration has the benefit of reduced cost due to the lack of need for additional measuring systems, the missing feedback of the table position means that the position control can only react inadequately to disturbances affecting the table, such as friction and process forces. In the area of machine tools with high demands on positioning accuracy, a linear measuring system is therefore commonly added to allow for a direct position control of the table position x_T [2]. In the setup under consideration, an absolute position measuring system integrated in the guide rails is used. For improved trajectory tracking the position controller is supplemented with a velocity feed-forward controller [16]. The controllers are parameterized for the experiments according to the common setting rules used in the machine tool sector. The velocity controller with the proportional gain K_p and the time constant T_n is set according to the principle of the symmetrical optimum and is computed at 8 kHz. The position controller operates at 1 kHz and the gain K_v is chosen in such a way that an overshoot-free positioning is achieved (aperiodic loop, damping ratio $\zeta = 1$) [17]. The corresponding parameters are listed in Table 2.

3 Experimental investigation of the transmission errors

In general gearing theory TEs denote the deviations between the position of the driving gear and that of the driven one [7]. For RPDs as a whole this definition is expanded accordingly. The rotary motion of the motor encoder θ_M is converted into the corresponding linear position x_M

$$x_M = \frac{\theta_M \cdot d_p}{2\, i_{PG}} \tag{1}$$

with the help of the gearbox transmission ratio i_{PG} and the pitch diameter of the pinion d_p. The difference between the linear position derived from the motor encoder x_M and the measured table position x_T is referred to as the TE

$$\mathrm{TE} = x_M - x_T \tag{2}$$

of the RPD in the following. The TE is initialized as zero at the beginning of the measurement window.

3.1 No-load transmission error

The TE of the system is firstly measured quasi-statically in no-load operation. Therefore, the table is moved with a velocity of 5 mm/s. In this way, dynamic effects can be excluded to solely observe the geometric deviations in the drive train. The table only has to overcome the friction that occurs in the system, which in this case is about 500 N. The measurement is carried out in both directions of travel.

Figure 4 shows the TE curves acquired. Basic characteristica are equally observed for both curves, which are composed of different independent sources of error. These individual effects have differing impact and are superimposed, thereby reinforcing or balancing each other out. Therefore, the specific composition of the cumulative error is highly individual and differs for each installation. Thus, the following discussion focuses on the quantification of the separate

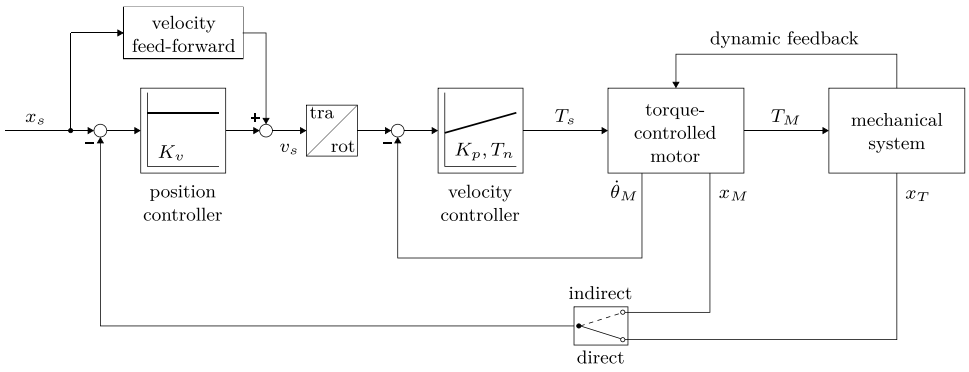

Fig. 3 Structure of a cascade control architecture for a feed drive based on [16]

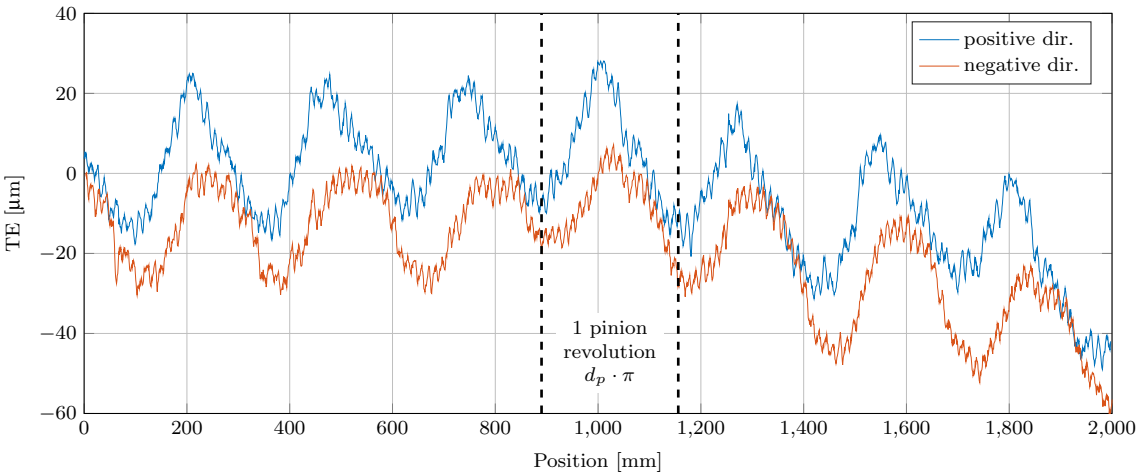

Fig. 4 No-load transmission error in both directions of movement

error components to evaluate their impact. For this purpose, different sources of error were measured and their influence on the TE was analyzed. The difference between the drive and the table is firstly subject to a drift. With constant motion of the motor, the table deviates from the corresponding ideal path. One reason for this, is the distance between the individual teeth of the rack being subject to manufacturing inaccuracies. During motion, these inaccuracies add up and result in a drift between the rotational movement of the pinion and the linear table movement. For the examined example, the accumulated pitch error over the measuring range amounts for up to 23 µm in positive direction and 44 µm in negative direction and thus contributes significantly to the position drift. Additional deviations are caused by tolerances in the alignment between racks and guide rails. Specifically, center distance and vertical alignment are subject to variation. For the system under consideration, the variation in center distance Δd was acquired by measuring the horizontal displacement of the racks perpendicular to the direction of movement. The observed deviation ranges up to 47 µm. Based on the gearing geometry, the resulting path deviation TE_d through shifting of the contact point is estimated to 18 µm by

$$\mathrm{TE}_d \approx \frac{\tan(\alpha_n)}{\cos(\beta)} \cdot \Delta d\,, \tag{3}$$

using the pressure angle α_n analog to the calculation of the radial gearing force [18]. The vertical alignment Δh, acquired by measuring the vertical displacement of the racks perpendicular to direction of movement, deviates up to 110 µm, resulting in path deviations TE_d of up to 39 µm, as given by

$$\mathrm{TE}_h \approx \tan(\beta) \cdot \Delta h\,. \tag{4}$$

The cause here likewise is the displacement of the contact point. Besides these deviations within the drive train, the measurement of the table position itself is also subject to inaccuracies. Tolerances in the alignment of the scale, pitch errors of the table measuring system as well as temperature variations can lead to deviations in the measurement of the distance travelled [19]. Due to the table measuring system being integrated in the guide rail, only the misalignment between it and the rack is a concern. While potentially relevant for long travel distances, over a distance of 2000 mm even a significant parallelism error of 2 mm only leads to a position deviation of 1 µm [19]. This source of error can therefore be neglected when referring to the magnitude of the observed drift. The accuracy of the measuring system itself is given by the manufacturer with ±5 µm per 1000 mm of travel for a temperature range of 0 – 70 ° C [20]. In summary, it can be stated that pitch errors of the rack, tolerances in the center distance and vertical alignment contribute to the total TE to a similar extent. The accuracy of the linear measuring system, albeit not negligible, is of minor significance. While pitch errors and measurement accuracy are predetermined through manufacturing, special attention should be paid to the alignment of the racks in order to minimize drift, especially when using an indirect position control. If the pitch errors of the individual rack elements are known, it is possible to arrange them in an order that keeps the total pitch error minimal.

Superimposed on the drift is a distinctly recognizable low-frequency oscillation in both runs. Its amplitude ranges from 20 to 40 µm and the period of 266.66 mm corresponds to one complete revolution of the pinion as per $d_p \cdot \pi$. The measurement results therefore suggest, that the errors are attributable to deviations in the rotary motion of the pinion respectively the gearbox output. An examination of the planetary gearbox revealed a periodic angular error of 11 m°

between input and output shaft over one full revolution of the pinion in both directions of motion. Coupled with the pitch diameter d_p, this results in a deviation of 8.1 µm in terms of the linear motion. In addition, alignment and manufacturing tolerances affect the rotational motion of the pinion and thus contribute to the TE. In the case under consideration, the pinion is welded onto the gear shaft and exhibits a radial runout of 12 µm, measured on the tooth tip at half the gear width. Complementary to this, the axial runout deviation, measured on the underside at the pitch circle, totals 25 µm. To estimate the corresponding effect on the TE, the vertical displacement caused by the axial runout is substituted into Eq. (4), resulting in a deviation of up to 9 µm. It is subsequently evident that both, the gearing in the gearbox and the runout characteristics of the pinion, have significant effects on the TE of the drive. It is therefore advisable to use high-quality gearboxes and to ensure that attention is paid to the alignment of the pinion on the output shaft. The established runout measurement in one plane should be supplemented by a second measurement in another plane in order to cover the rotational properties more precise.

In addition to the low-frequent periodic error, there is another, higher-frequency one superimposed. Its amplitude is in the single-digit µm range and its period corresponds to the meshing frequency of the rack and pinion, which, corresponding to the number of teeth z, is higher by a factor of 20 than that of the pinion revolutions. This error component can therefore be attributed to deviations of the tooth flank geometry from the ideal involute shape. One reason for such deviations are unavoidable tolerances in the manufacturing process of the gearing components. The typical magnitude of these tolerances corresponds with the observed errors [21]. However, there are also specifically intended modifications of the tooth flank shape [22]. Such tooth flank modifications are primarily used to reduce stress peaks under load and consequently improve the load capacity. The gearing thus is designated for a specific load condition. The tooth flanks that deviate from the ideal shape in the load-free state then deform in such a way that optimal load distribution and motion uniformity are achieved under nominal load [12]. This effect can be observed for the meshing of the RPD under investigation, which becomes clear in Sect. 3.2. For operating conditions with loads differing from the optimized range, this results in an added TE for tooth meshing, which typically falls within the range of the deviations observed in the example [23].

While the error components just discussed are directly evident from the TE graphs, there are several others. While their effect on the TE of the system is negligible in terms of the resulting position deviations, they nevertheless represent an excitation of the system, especially when they occur periodically. For further investigation, the recorded TEs are transformed into the frequency domain. Figure 5 shows the resulting diagram.

The x-axis is not scaled by the frequency f in Hz, but has been normalized to full pinion revolutions n using the velocity v according to

$$n = f \cdot \frac{\pi \cdot d_p}{v}. \tag{5}$$

In this way, the error spectrum is detached from the velocity and the individual components can be assigned to their sources. Thus, the distinct peak at the value 1 corresponds with the full pinion revolutions and the the one at factor 20 correlates with the number of teeth z. Moreover, for both directions of travel, peaks appear at factors 4.27 and 6.67. The odd multiples of the pinion revolutions indicate that the causes are to be found in the translational movement of the drive. The corresponding conversion using the pitch circle of the pinion as in Eq. (1) results in a period of 62.5 mm and 40 mm, which corresponds to the bore spacing of the rack and the guide rails, respectively. Due to the punctual mounting of the components, their stiffness fluctuates, leading to varying degrees of deformation and thus positional oscillations [13].

In terms of further rotational deviations besides the expected harmonics, there is one distinct high-frequency

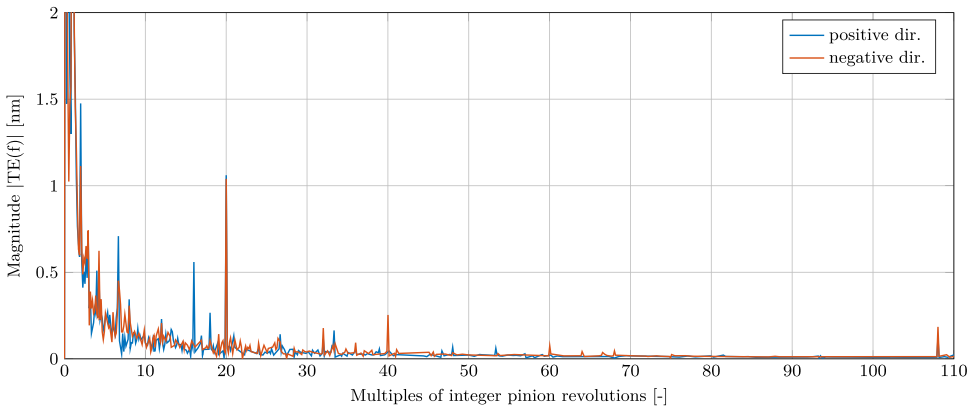

Fig. 5 Frequency spectrum of the no-load transmission error in both directions of movement

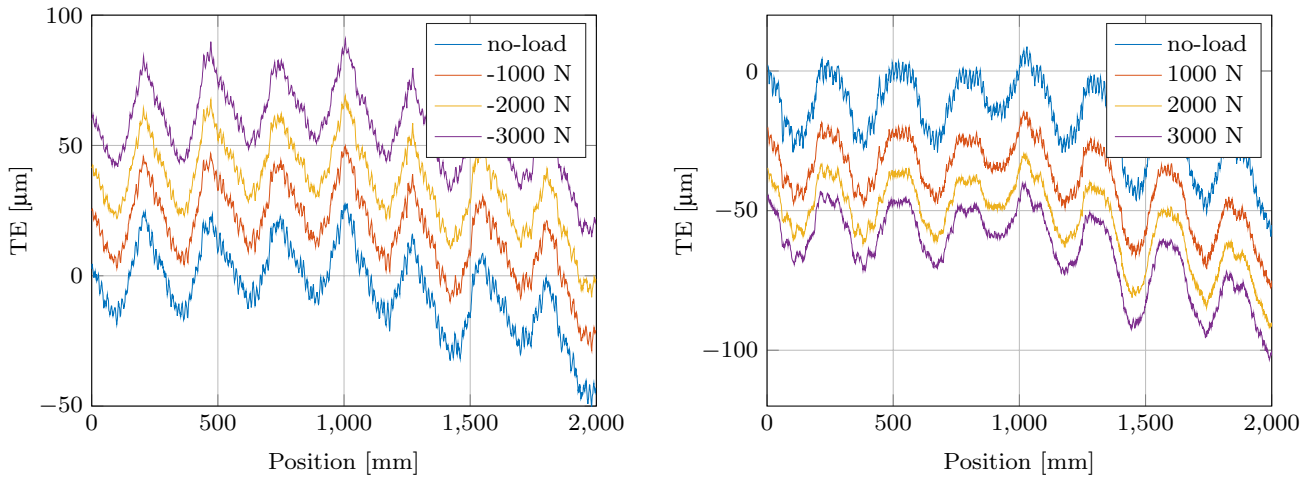

(a) Positive direction of movement

(b) Negative direction of movement

Fig. 6 TE of the RPD under varying loads

peak at factor 108. This excitation correlates with the number of teeth of the hollow ring of the output stage of the planetary gearbox. Furthermore, the influence of the motor is also evident, although only in the positive direction of travel. The revolutions of the motor respectively the gearbox input shaft appear at a factor of 16, which corresponds to the total transmission ratio of the gearbox i. The explanation for the strongly direction-dependent appearance will be discussed later. First, the effects of varying loads on the TEs are examined.

3.2 Investigations under load

The approach to the investigations under load largely complies with the prior measurements. The only difference are constant forces applied by the LDD contrary to the direction of travel. The results are presented in Fig. 6.

The diagrams show the resulting TEs in load-free condition and with 1000 N, 2000 N and 3000 N counterforce on top of the friction. It becomes apparent that there is a constant offset between the individual curves, which corresponds to the static deformation of the mechanical system under the constant load. The corresponding average stiffness for the observed range of forces is 48.5 N/µm in positive and 64.1 N/µm in negative direction of movement. In addition, there is a considerable alteration of the TEs with increasing load, particularly in the negative direction of movement. While the basic shape including drift and low-frequency oscillation remains unchanged, the amplitude of the errors with tooth meshing frequency decreases significantly. This is due to the deformations of the tooth flanks in conjunction with the profile modifications described in Sect. 3.1. The geometric deviations in the load-free state

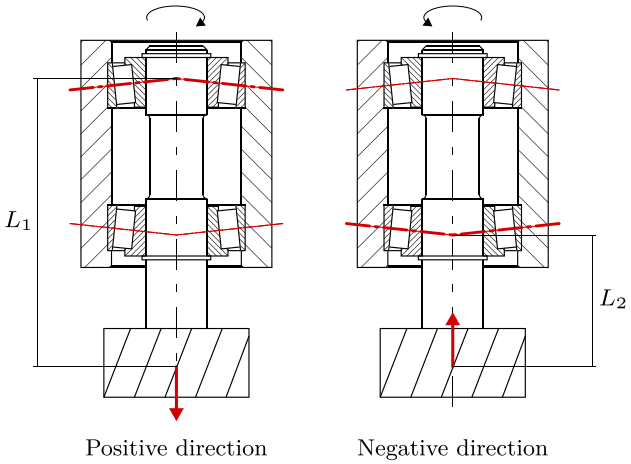

Fig. 7 Angular contact bearing assembly under axial loads with different direction

converge to the ideal involute shape under load and the uniformity of motion improves.

A relevant consideration at this point is, that counterforce on the gearing does not inevitably arise from external sources. As mentioned in Sect. 1, in practical implementations two drives are typically preloaded against each other to minimize backlash. In terms of the individual drives the origin of the counterforce is irrelevant and a constant preload results in an additional force offset to the load. However, the extent to which the TEs of the individual drives interfere with each other is subject of future research.

While a substantial decrease in the amplitude can be observed for the negative direction of travel, the difference is more subtle for the positive direction. This and other noticeable direction-dependent characteristics are a specific property of RPDs [2]. The reason for this is to be sought in the meshing of the rack and the pinion. As

mentioned before, most gears are designed with helical teeth to achieve smoother motion and higher contact ratio. Such helical toothing leads to considerable axial forces along the gearbox shaft. For the present helix angle β, a tangential load F_{load} of 3000 N according to

$$F_{ax} = F_{load} \cdot \tan(\beta) \tag{6}$$

leads to an axial force F_{ax} of 1064 N acting on bearings and supports. In order to be capable of withstanding these forces, the output shaft of the gearbox is commonly carried by angular contact bearings. Figure 7 illustrates such an assembly by the example of a back to back arrangement of tapered roller bearings.

It is evident that the complementary inclinations of the bearing planes lead to a differing distribution of forces depending on the direction of the axial force. As a consequence, the resulting tangential and axial forces are largely absorbed by one of the two bearings in each case, depending on the direction of travel. The mounting arrangement of the bearings results in different leverage and hence differing stiffness and tilting rigidity. In conjunction with the inevitable hysteresis and potential backlash of the bearing, a direction-dependent vertical shift of the pinion occurs [24]. The resulting change of the contact conditions of the gearing produces the observed discrepancies between the two directions of travel of the feed drive [25].

The phenomenon just described does not only apply to the rack and pinion, but can also be transferred to the gearbox, which utilizes helical gearing as well. Thus, the direction-dependent occurrence of the motor revolutions observed in the frequency spectrum in Fig. 5 can also be traced back to changed contact conditions. As the preceding considerations indicate, the heavily direction-dependent characteristics of RPDs are intrinsically linked to the design and functional principle of such drives. However, constructive efforts can be made to reduce consequences for the accuracy. Stiffer or preloaded bearings can decrease the resulting displacements. In addition, consideration should be made regarding the direction-dependent behavior of the drive, when defining the helix angle. For high accuracy, the resulting axial forces should be kept as low as feasible.

4 Impact on the position controlled drive

The aim for the following measurements is to investigate to what extent the TEs can be compensated by the position controller. For this purpose, several load-free measurements were carried out in negative direction of motion. Among the individual runs the constant velocity is varied in fixed steps from a reference v_{ref} of 180 mm/s. Since the friction is velocity dependent, it totals about 1150 N for v_{ref} and alters by ± 250 N for the maximum resp. minimum velocity displayed. While consequently a load change is encountered, it is of negligible magnitude compared to the forces necessary to alter the transmission characteristics of the drive as displayed in Fig. 6. The control error between target trajectory and measured table position is observed in Fig. 8. The position range has been reduced for a more detailed illustration.

While the drift is not observable, the periodic position errors described above are represented in the control error. It is evident that the position controller is incapable of thoroughly compensating for the TEs.

However, a velocity dependency becomes apparent in this context. The amplitude of the high-frequency deviations with tooth meshing frequency increases with increasing velocity. In addition, the low-frequency oscillations per pinion revolution are suppressed for low velocities, but are present in the control error for higher velocities. While the individual error components in Fig. 5 are normalized by Eq. (1), the fundamental frequencies of the TEs scale proportionally to the drive velocity. As a result, the derivatives of the position errors also increase. Since these velocity errors can only be registered by the position measuring system of the table, they are not part of the highly dynamic velocity control loop. Thus, instead of an immediate suppression of the occurring velocity deviations, only the subsequent position errors are registered and compensated. The resulting time delay is the cause of the unsatisfactory suppression of the TEs.

4.1 Excitation of natural frequencies

The measurement run for the velocity of $0.75\, v_{ref}$ in Fig. 8 reveals an unexpected response. A significant high-frequency oscillation dominates the control error. The velocity dependent occurrence suggests the excitation of a natural frequency of the system. To verify this, the position errors for several velocities are transformed into the frequency domain, as shown in Fig. 9.

This diagram illustrates how the error components of the TE shift in relation to the velocity, the corresponding dominant peaks move along the frequency axis proportionally. In the proximity of 50 Hz, however, excitations appear for all measurement runs. This fixed frequency correlates with the first mechanical eigenfrequency of 53 Hz as shown in the frequency response of the mechanical system in Fig. 10. The distinct oscillations for the considered velocity $v = 0.75\, v_{ref} = 135$ mm/s in Fig. 8 are due to this eigenfrequency as it is evident by the dominant peak in Fig. 9. To investigate the correlation with the TEs, Eq. (5) is inverted. Thus, the error components identified in Fig. 5 can be assigned to the corresponding frequencies for the specified velocity. For the factor $n = 108$ of the gearing within the output stage of the gearbox, this frequency

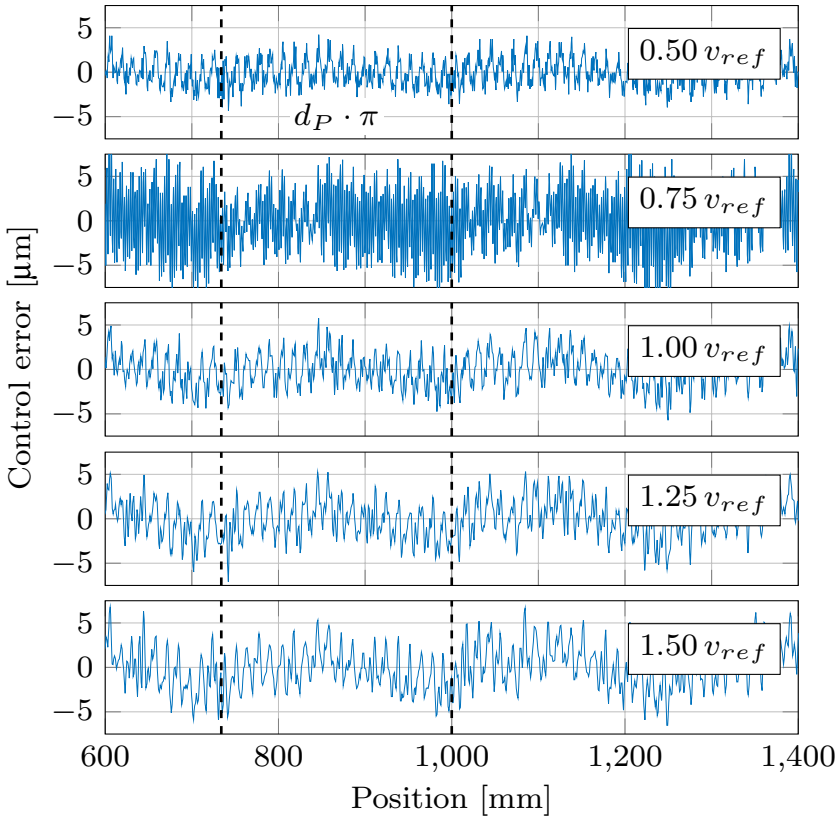

Fig. 8 Control error of the position controlled table for different velocities

$$f = \frac{n \cdot v}{\pi \cdot d_p} = \frac{108 \cdot 135\ \text{mm/s}}{\pi \cdot 84.882\ \text{mm}} = 54.7\ \text{Hz} \tag{7}$$

coincides with the mechanical eigenfrequency. The two excitations subsequently reinforce each other and cause the observed position oscillations.

It is evident that the periodically occurring parts of the TE cannot only result in respective position deviations. Due to the varying frequency determined by the velocity, they coincide and interfere with natural frequencies of the system in certain cases. However, the affected states of operation can be identified and avoided, if the natural frequency of the system is known. The dominant TE components can be identified through transformation into the frequency domain as in Fig. 5 and the corresponding frequencies can be derived for all drive velocities utilizing Eq. (5). The velocity ranges in which one of these falls within the scope of a natural frequency should be avoided in operation. In addition, this issue should be taken into account during the design phase. In particular, the use of multi-stage gearboxes multiplies

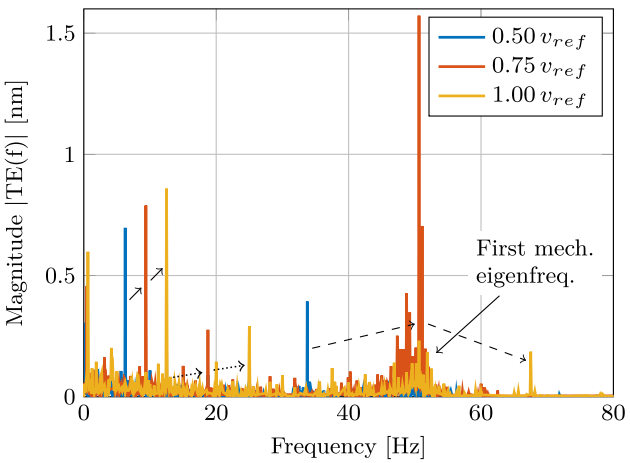

Fig. 9 Frequency spectrum of the TE for different velocities

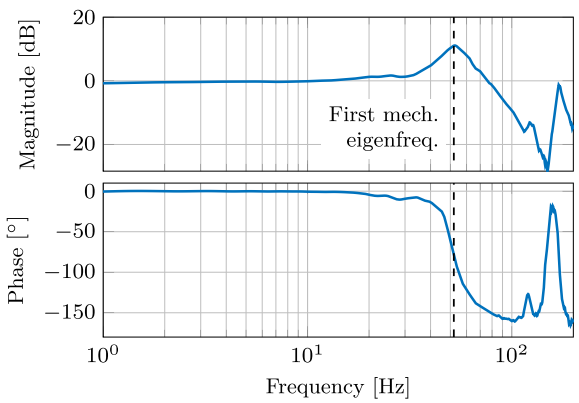

Fig. 10 Frequency response of the drive mechanics

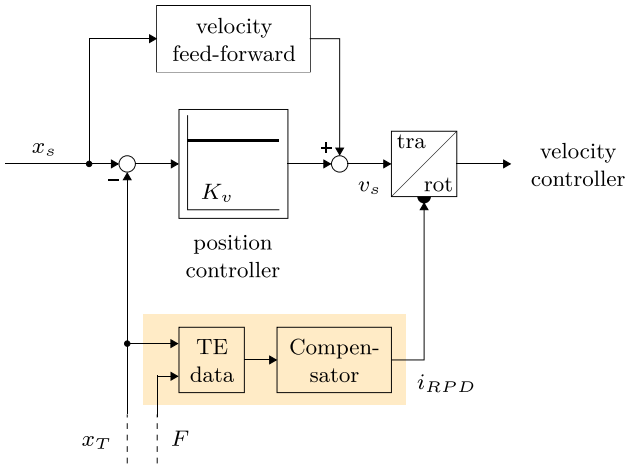

Fig. 11 Implementation of the TE compensation in the drive control scheme

the number of excitations induced in the system and should therefore be carefully considered.

5 Error compensation

In the previous sections, it became apparent that the TEs have a significant impact on the accuracy of RPDs. However, the knowledge gained can be used to compensate for the deviations by adaptation of the control scheme. For this purpose, the TEs of the individual system are systematically recorded. As shown in the previous sections, the TE depends on the position and load. The acquisition of the error curve in the load-free state can be carried out during commissioning, whereas the defined loads required to observe the load-dependent error curves cannot be realized without special measurement setups. Instead, the data can be acquired during operation. For this purpose, the position difference between the motor and the table is recorded analog to Fig. 6, while the load is determined using the motor torque.

The data then is processed to allow the compensator to retrieve the appropriate TE in real-time based on the position and load. In addition, it must be taken into account that the position changes continuously through the table motion, while the load in most cases changes erratically. The method used therefore has to interpolate between the discrete load states. Various approaches exist for this purpose. One option is to store the TEs in the form of a two-dimensional look-up-table (LUT) across position and load. While this method is straightforward to implement, the processing time as well as the requirement to define the interpolation strategy are disadvantageous. Furthermore, additional signal processing is required to recognize redundant states and process the corresponding measured TE values, e.g. by averaging, and to convert the data into a tabular form. Regression algorithms developed in the field of machine learning can automate these steps and offer further advantages. Regression trees, for instance, structure the data sets in an offline optimization to minimize processing time during operation. The optimization automatically clusters the data of redundant states and can be executed in a deterministic manner, so that this approach represents a more advanced alternative to LUTs. It is also feasible to represent the data using neural networks, which can improve the inter- and extrapolation for unknown load states through their capability of abstraction.

In addition to the acquisition of the TE data, the integration of a compensator into the drive control represents a further challenge. The approach presented in the following is applicable for all data processing concepts just described. The insufficient compensation of the TEs by the position control is caused by the transmission ratio assumed to be ideal for the conversion between the linear position and rotational velocity controller. Utilizing the TE data, it is possible to provide an adaptation to the real environment instead. Based on Eq. 1 and Eq. 2, the real transmission ratio i_{RPD}

$$\begin{aligned} i_{RPD}(x_T, F) &= \frac{\dot{\theta}_M}{\dot{x}_T} = \frac{\dot{x}_M}{\dot{x}_T} \cdot \frac{2\, i_{PG}}{d_p} \\ &= \frac{\dot{x}_T + \frac{d\,\mathrm{TE}(x_T,F)}{dt}}{\frac{d\,x_T}{dt}} \cdot \frac{2\, i_{PG}}{d_p} \\ &= \left(1 + \frac{d\,\mathrm{TE}(x_T, F)}{d\,x_T}\right) \cdot \frac{2\, i_{PG}}{d_p} \end{aligned} \tag{8}$$

can be calculated using the position x_T and a constant load F. It is evident, that i_{RPD} correlates with the TE derived with respect to the table position. The momentary transmission ratio calculated in this manner is then used within the closed-loop control, as shown in Fig. 11, thereby compensating for the TEs.

6 Conclusion

In this paper, investigations of the transmission errors of rack-and-pinion drives are conducted. This is carried out using a test bench that is equivalent to common implementations in the machine tool sector. Through examination of the position errors occurring in the drive train of rack-and-pinion drives in load-free operation, it is shown that the table position is subject to a significant drift as well as periodic errors with the frequency of the pinion revolutions and the meshing of the teeth. The effect of the individual error sources on the transmission error is discussed and quantified. Investigations in the frequency domain reveal further error components that

are assigned to their mechanical sources. Thus, in addition to rack and pinion, other components of the drive train, such as the gearbox and the guide rails, also have an effect on the transmission behaviour.

Based on the investigations of these basic characteristics, changes of the transmission errors under load are examined. The application of defined counterforces leads to deformations of the tooth flanks, resulting in an alteration of the transmission error. The highly direction-dependent characteristics of rack-and-pinion drives are particularly noticeable in this context. The load distribution of the helical gearing in conjunction with the construction of the drive system is identified as the central cause of this.

Experiments with a direct position control demonstrate that the transmission errors cause significant trajectory tracking errors even at moderate velocities. This problem intensifies with increasing velocity and the error magnitudes continue to increase. It also emerges that, in addition to the obvious position errors, the excitation of the machine structure caused by periodic errors is likewise a concern.

Based on the analysis of the transmission errors, potential compensation schemes using direct position measurement are discussed.

Current research is concerned with the experimental validation and comparison of the outlined compensation concepts. In addition, the findings obtained for a single drive will be validated with electrically preloaded drives.

Acknowledgements This work was funded by the Deutsche Forschungsgemeinschaft (DFG, German Research Foundation), Project No. 447112572. The authors gratefully acknowledge the support by DFG.

Funding Open Access funding enabled and organized by Projekt DEAL.

Declarations

Conflict of interest The authors declare that they have no conflict of interest.

References

1. Uriarte L, Zatarain M, Axinte D, Yagüe-Fabra J, Ihlenfeldt S, Eguia J, Olarra A (2013) Machine tools for large parts. CIRP Ann 62(2):731–750
2. Engelberth T (2020) Adaptive Verspannung von Zahnstange-Ritzel-Antrieben. Dissertation, Universität Stuttgart
3. Altintas Y, Verl A, Brecher C, Uriarte L, Pritschow G (2011) Machine tool feed drives. CIRP Ann 60(2):779–796
4. Engelberth T, Apprich S, Friedrich J, Coupek D, Lechler A (2015) Properties of electrically preloaded rack-and-pinion drives. Prod Eng 9(2):269–276
5. Karim A, Lindner P, Verl A (2018) Control-based compensation of friction and backlash within rack-and-pinion drives. Prod Eng 12(5):589–596
6. Brenner F, Lechler A, Verl A (2021) Acceleration-based disturbance compensation for elastic rack-and-pinion drives. Prod Eng 15:791–800
7. Philippe V (2012) On the modelling of spur and helical gear dynamic behaviour. In: Gokcek M (ed) Mechanical engineering. InTech, London
8. Velex P, Maatar M (1996) A mathematical model for analyzing the influence of shape deviations and mounting errors on gear dynamic behaviour. J Sound Vib 191(5):629–660
9. Heider MK (2012) Schwingungsverhalten von Zahnradgetrieben. Dissertation, TU München
10. Rao SS, Yoon KY (2001) Minimization of transmission error in helical gears. Proc Inst Mech Eng Part C J Mech Eng Sci 215(4):447–459
11. Cooley CG, Parker RG (2014) A review of planetary and epicyclic gear dynamics and vibrations research. Appl Mech Rev 66(4):040804
12. Chen Z, Zeng M, Fuentes-Aznar A (2020) Geometric design, meshing simulation, and stress analysis of pure rolling rack and pinion mechanisms. J Mech Des 142(3):031122
13. Hoffmann F (2008) Optimierung der dynamischen Bahngenauigkeit von Werkzeugmaschinen mit der Mehrkörpersimulation. Dissertation, RWTH Aachen
14. D Marano, A Piantoni, L Tabaglio, M Lucchi, F Pellicano (2017) Effects of gear manufacturing errors on rack and pinion steering meshing. In: First World congress on condition monitoring
15. Duchemin M, Collee V (2016) Profile optimization of the teeth of the double rack-and-pinion gear mechanism in the mce-5 vcri engine. SAE Int J Engines 9(3):1786–1794
16. Zirn O (2008) Machine tool analysis: modelling, simulation and control of machine tool manipulators. Habilitation thesis, ETH Zurich
17. Schröder D (2015) Elektrische Antriebe—Regelung von Antriebssystemen. Springer, Berlin
18. Vullo V (2020) Gears: volume 1: geometric and kinematic design, vol 10, 1st edn. Springer, Cham
19. ISO 230-2 (2011) Test code for machine tools—part 2: determination of accuracy and repeatability of positioning numerically controlled axes. International Organization for Standardization, Geneva
20. Schneeberger GmbH (2021) Application catalog MONORAIL and AMS. www.schneeberger.com/fileadmin/documents/downloadcenter/01_product_catalogues_company_brochures/01_Linear-_and_profiled_guideways/01_MONORAIL_and_AMS/MONORIAL_and_AMS_Application_catalog_EN.pdf. Accessed 10 Aug 2021
21. ISO 1328-1 (2013) Cylindrical gears—ISO system of flank tolerance classification—part 1: definitions and allowable values of deviations relevant to flanks of gear teeth. International Organization for Standardization, Geneva

22. ISO 21771 (2007) Gears—cylindrical involute gears and gear pairs—concepts and geometry. International Organization for Standardization, Geneva
23. Kissling U (2010) Effects of profile corrections on peak-to-peak transmission error. Gear Technology 27(5):52–61
24. Roda-Casanova V, Sanchez-Marin F (2017) Contribution of the deflection of tapered roller bearings to the misalignment of the pinion in a pinion-rack transmission. Mech Mach Theory 109:78–94
25. Jiang H, Shao Y, Mechefske CK, Chen X (2015) The influence of mesh misalignment on the dynamic characteristics of helical gears including sliding friction. J Mech Sci Technol 29(11):4563–4573